EASR

Engineering and Applied Science Research

https://www.tci-thaijo.org/index.php/easr/index

Published by the Faculty of Engineering, Khon Kaen University, Thailand

Investigation on the CdS-incorporated decorated TiO_2 nanoporous arrays as a photoanode for cathodic protection of 304 SS in a 0.5 M NaCl solution

Aleena Boonserm, Chaiyaput Kruehong, Apichart Artnaseaw, Panomkorn Kwakhong and Varinrumpai Seithtanabutara*

Department of Chemical Engineering, Faculty of Engineering, Khon Kaen University, Khon Kaen, 40002, Thailand

Received August 2016
Accepted September 2016

Abstract

A CdS-incorporated TiO_2 nanoporous material was fabricated using an anodic oxidation method combined with a chemical bath deposition technique. The three steps of anodization were completed to grow the anodic TiO_2 nanoporous arrays (TNPs) on a titanium sheet in an ethylene glycol electrolyte containing 0.38wt% NH_4F with the addition of 1.79 wt% H_2O under an applied potential of 40 V. The CdS-decorated TiO_2 nanoporous arrays (CdS/TNPs) were prepared using five dipping cycles of CdS deposition on the TNPs sample, which was calcined at 600°C in air for 3 h at a heating rate of 5 °C min^{-1}. The structure and composition of the as-prepared TNPs and CdS/TNPs were characterized using field emission scanning electron microscopy, X-ray diffraction and energy dispersive X-ray spectroscopy. The photoelectrochemical performance of the TNPs and CdS/TNPs electrode in a 0.5 M NaCl solution was evaluated through the electrochemical measurements under illumination and dark conditions. Decoration of CdS onto the TiO_2 nanoporous array gave a higher transient photocurrent indicating a higher separation efficiency of the photogenerated electron-hole pairs and facile transport of these electrons to the metal substrate. Compared to a bare TiO_2 nanoporous array, the CdS/TNPs photoanode exhibited more effective photocathodic protection properties for 304 stainless steel (304SS) under visible light illumination, with a photopotential of -412 mV versus silver-silver chloride electrode (SSE). This indicates that CdS has an enhanced effect on the photogenerated cathodic protection of TiO_2 nanoporous array for 304SS.

Keywords: Anodization, Titanium dioxide, CdS, Nanoporous, Cathodic protection

1. Introduction

Corrosion is an electrochemical reaction process that causes damaging to metals and makes rust on metallic compounds. This is mainly caused by the interaction between the metal surface and its environment, i.e., air, water or moisture. 304 stainless steel (304SS) is the most widely used steel of its type due to its low cost and outstanding physical properties: high corrosion resistance, high strength and elongation. However, 304SS has a limitation in chloride ion solutions as pitting corrosion can occur rapidly on its surface [1]. Thus, the intensive efforts to develop anticorrosion surface pretreatments and coating techniques for 304SS have been investigated [2-3]. It was found that coating surfaces of the metal with a titanium dioxide (TiO_2) film can increase the corrosion resistance of this metal under illumination [4]. Recently, a TiO_2 coating or coupling to a metallic substrate exposed to visible light irradiation has been developed for photocathodic protection with the principle of photogenerated electron-hole pair separation [5-6]. These excited electrons can be easily transported from a TiO_2 film to the coupling metal. Thereby, the photopotential shifts to a more negative value than the original corrosion potential in an environment, indicating that the metal is still protected. Ordered-nanoporous TiO_2 with a high specific surface area is simply fabricated by a direct electrochemical oxidation method. The mobile electrons of the anodic TiO_2 nanofilm can be more easily excited than those of films prepared using the other methods. Therefore, an anodic nanosized-TiO_2 electrode can be suitably used in the cathodic protection of a metal substrate [7]. However, pure TiO_2 can be induced only by ultraviolet light at a wavelength of about 380 nm or less because of its intrinsic wide bandgap (3.2 eV for anatase and 3.0 eV for rutile). So, its practical application has been limited by the excitation light source. Moreover, a fast electron-hole recombination rate of the photogenerated electron-hole pairs will decrease the photoelectric conversion efficiency of TiO_2, so that cathodic protection is difficult to maintain in the dark [8]. To extend the photoresponse into the visible region and improve the charge separation of electron-hole pairs, several investigations have been done on the modification of TiO_2 films. For photochemical corrosion protection, the metal is galvanically coupled with a semiconductor that has a conduction band potential that is more negative than the corrosion potential of the protected metal. The photogenerated electrons are transferred from the semiconductor to the metal substrate, resulting in a shifting

*Corresponding author: Tel.: +66 4336 2240
Email address: tmallika@kku.ac.th
doi: 10.14456/easr.2017.10

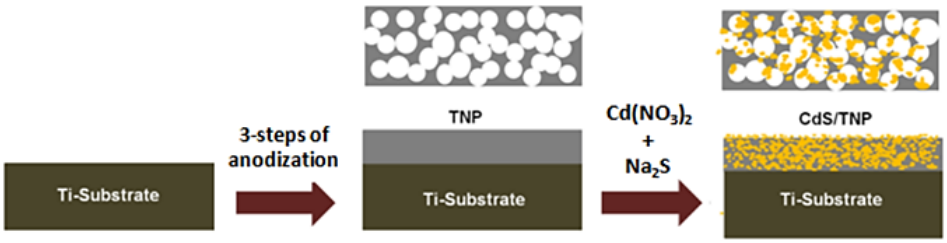

Figure 1 Schematic diagram of the procedure for preparing the CdS/TNPs.

of the metal potential. Semiconductor-doped TiO_2 has been widely evaluated for this purpose. Generally, some semiconductors such as $SrTiO_3$ [9], WO_3 [10], SnO_2 [11], PbS [12], CdS [13-15], CdSe [16] and CdTe [17-18] have been doped into TiO_2 films.

Based on its narrow band (2.4 eV) and good photoelectric properties, CdS has been used in photocatalytic degradation of water pollutants [15, 19] and in electronic devices. The introduction of CdS into a TiO_2 film extends the light harvesting capability of a TiO_2 electrode into the visible region [20]. Preparation of a CdS/TiO_2 composite film can be done using different methods. A CdS/TiO_2 composite film prepared by electrodeposition has low photo-to-current efficiency and contains agglomerated CdS, because it has been carried out at a higher temperature (100 °C) [21]. A sonoelectrochemical method was developed to fabricate a CdS/TiO_2 composite film at a lower temperature (50 °C). Moreover, this film can absorb light in the visible region [22]. The simple and convenient technique is a chemical bath deposition, done by dipping TiO_2 film in a CdS solution at room temperature [19, 23].

There are a few reports on decoration of TiO_2 with CdS for photocathodic protection [13-15]. In this work, TiO_2 nanoporous arrays (TNPs) were fabricated by electrochemical oxidation of a titanium substrate in an ethylene glycol electrolyte containing 0.38 wt% NH_4F with the addition of 1.79 wt% H_2O under an applied potential of 40 V. Then CdS was decorated onto the as-prepared TNPs by chemical bath deposition. The photoelectrochemical properties of TNPs photoanodes before and after CdS-doping were investigated. Their cathodic protection activities of 304SS were examined under visible light illumination and dark conditions in 0.5 M NaCl.

2. Materials and methods

2.1 Preparation of TiO_2 nanoporous arrays (TNPs)

Ti sheets (purity>99%) with dimensions of 2 cm x 2 cm x 0.1 cm were polished in an acid mixture of HF (49%) and HNO_3 (70%) with a mixing ratio of 25:75 by volume. The anodization experiments were carried out in a two-electrode cell called a BCC as presented in a previous study [24]. Anodic films were grown from the surface of a Ti specimen in an ethylene glycol electrolyte containing 0.38 wt% NH_4F with the addition of 1.79 wt% H_2O at 40 V. A three-step anodization was used as previously described [25]. The 1st and 2nd steps were done with anodizing times of 1 and 2 h, respectively, and the 3rd step was completed 3 h afterwards. The oxide film formed during the previous step was tape removed and washed with DI water before being re-anodized in the next step. After anodization, the sample was rinsed with DI water and dried in air at room temperature. The amorphous films, with area of 2 cm^2 attached on the titanium substrate, were annealed at 600 °C in air for 3 h using a heating rate of 5 °C min^{-1} and naturally cooled to room temperature.

2.2 Synthesis of CdS-decorated TiO_2 nanoporous arrays (CdS/TNPs)

A chemical bath deposition method described elsewhere [23] was applied for doping CdS onto a TiO_2 nanoporous array. In detail, the anodized TiO_2 nanoporous specimen was immersed in a 0.4 M $Cd(NO_3)_2$ ethanol solution and then a 0.1 M Na_2S methanol solution for 1 min at each immersion step. The specimen was rinsed with ethanol between these steps and this was done five times. Finally, the CdS/TNPs specimens were air dried at room temperature for subsequent use. The procedure for the preparation of CdS/TNPs is shown in Figure 1.

2.3 Characterization

The surface morphologies of samples were observed using a field emission scanning electron microscope (FE-SEM, JSM-7800F) operated at 15 kV. The cystallinity of the TNPs was identified by X-ray diffraction (D8 Advance Bruker XRD, CuKα radiation with λ=1.5406°A) at a scanning rate of 10° min^{-1}, and 2θ ranging from 20° to 80°. The chemical composition of TNPs and CdS/TNPs were detected using an Oxford Instrument Energy Dispersive X-ray Spectroscopy (EDS).

2.4 Photoelectrochemical measurement

The photoelectrochemical behavior of the as-prepared photoanodes (TNPs or CdS/TNPs) was determined using a Gamry 600 Potentiostat-Galvanostatic system under the visible light illumination of an 11W compact florescence lamp (Sylvania, Daylight 865, λ > 400 nm). All tests were done using a custom-made three-electrode experimental system in 0.5 M NaCl solution at 25°C. For photocurrent spectral measurements, the TNPs or a CdS/TNPs/Ti sheet served as the working electrode (WE), while a platinum plate (0.5 cm x 0.5 cm x 0.1 cm) and an Ag/AgCl (0.5 cm x 2 cm x 0.1 cm) served as the counter electrode (CE) and the reference electrode (RE), respectively. Herein, the electrode potentials were measured using a saturated KCl/AgCl/Ag electrode (silver-silver chloride electrode, SSE). The polarisation curves were determined at a scan rate of 2 mV s^{-1}. Photocurrents of the prepared films were measured in the presence and absence of illumination at an applied potential of 0 V versus SSE. To investigate the photocathodic protection performance, the photoanode was galvanically coupled with a 304 stainless steel sample (304SS, 2.5 cm x 5 cm x 0.1 cm). Before an anticorrosion test, the 304SS specimen was double polished with 600 and 1200 grit sand paper to remove the native oxide and to obtain smooth surfaces. The metal was ultrasonically cleaned in ethanol and

then DI water for 10 min at each step. The TNPs or CdS/TNPs, 304SS and Ag/AgCl served as a working electrode (WE), counter electrode (CE) and reference electrode (RE), respectively. The filmed-side of photoanode faced towards the irradiation, and the area ratio between the specimen and 304SS was kept at 5:1, as shown in the experimental setup (Figure 2).

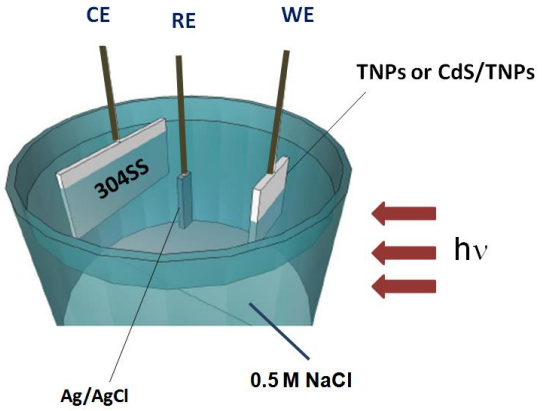

Figure 2 Schematic illustration of the experimental setup for photoelectrochemical measurements.

3. Results and discussion

3.1 The morphologies and crystal structures of the TNPs and CdS/TNPs photoelecrodes

Figure 3a shows the top-view morphologies of a pure TNPs array formed on the titanium sheet during three anodization steps at an applied potential of 40 V in an ethylene glycol electrolyte containing 0.38 wt% NH_4F with the addition of 1.79 wt% H_2O. It could be observed that the TiO_2 nanoporous arrays reveal a high-density of honey-comb hexagonal microstructure with non-uniform pores having an average pore size of about 75 nm. Figure 3b shows FE-SEM images of the CdS/TNPs after CdS deposition after 5 dipping cycles.

CdS nanocrystals were incorporated into the TNPs and extensively covered the outer surface. The composition of the CdS/TNPs was determined using Energy Dispersive X-ray Spectroscopy (EDS). The EDS spectrum of CdS/TNP (Figure 3c and 3d) revealed the peaks of Ti, O, Cd and S with weight ratios of 48.77%, 39.24%, 9.28% and 2.71%, respectively. The Ti and O peaks are from TNPs, while the Cd and S peaks resulted from CdS nanoparticles. The deposited materials are CdS because the atomic ratio of Cd to S is close to unity [13].

The FE-SEM observations were confirmed by the XRD spectra as shown in Figure 4. Here, only the peaks corresponding to titanium metal are seen (curve a). After calcination at 600°C in air for 3 hr, the annealed TNPs sample showed characteristic diffraction peaks (curve b) at 25.27°, 37.70°, 47.98°, 53.30° and 54.99°, corresponding to the anatase phase of TiO_2 (JCVPDF 89-2762). The intensity of anatase TiO_2 crytallite was found to be about 75.70%. For the CdS/TNPs prepared using a 5 cycle chemical bath deposition method (curve c), the diffraction peaks of CdS occurred at 26.6°, 28.3° and 43.9°, indicating a hexagonal structure with crystal faces of (002), (101) and (110).

3.2 Photochemical performances of the TNPs and CdS/TNPs photoelecrodes

The charge separation efficiency in the electrode and the effective separation of photogenerated electron-hole pairs were evaluated using the photocurrent. The transient photocurrent response of electrodes was measured by periodically interrupting the visible white light illumination. Figure 5 shows the current-time (i-t) characteristics of the

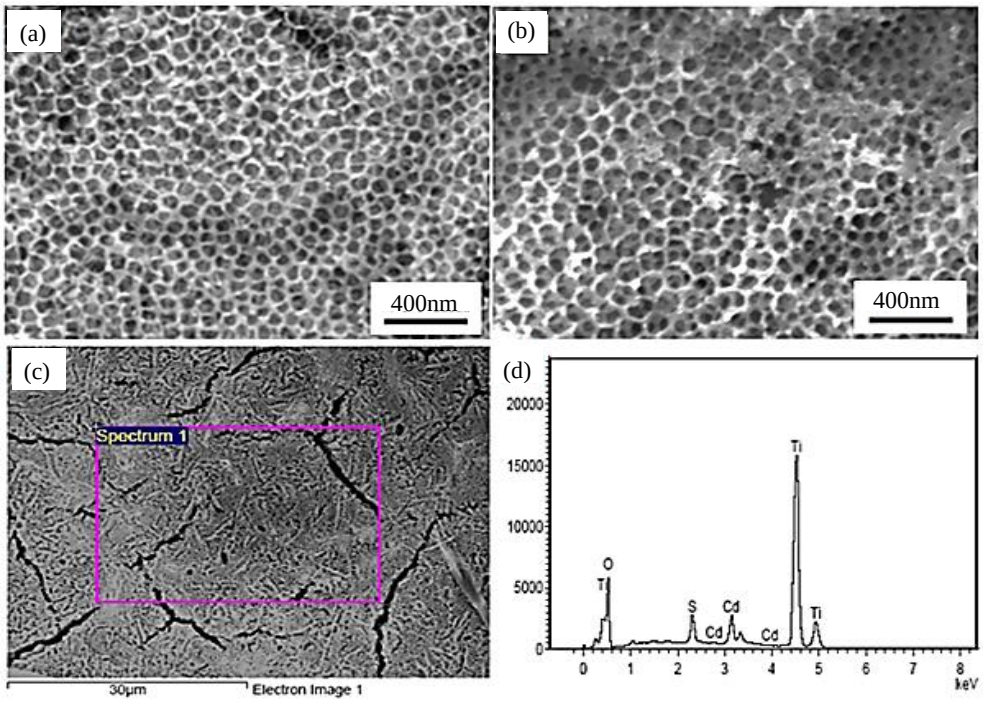

Figure 3 (a) Top view FE-SEM image of the TNPs, (b) Top view FE-SEM image of the CdS/TNPs, and the corresponding area of the CdS/TNPs (c) was investigated as EDS spectrum (d).

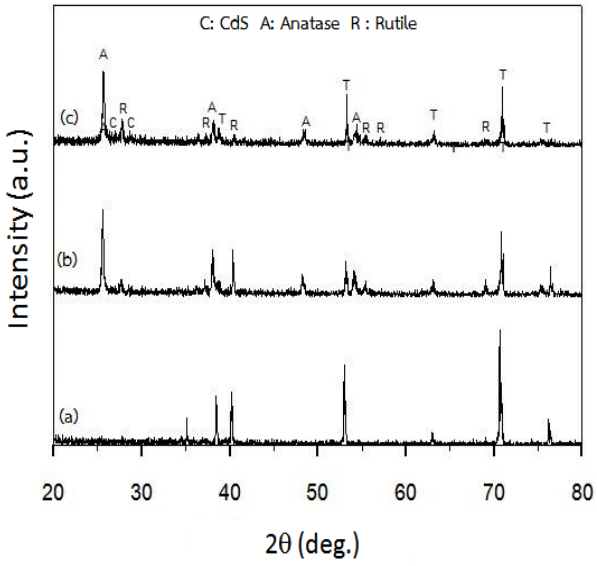

Figure 4 XRD spectra of (a) Ti substrate, (b) annealed TNP at 600°C and (c) CdS/TNPs after CdS chemical bath deposition for five cycles.

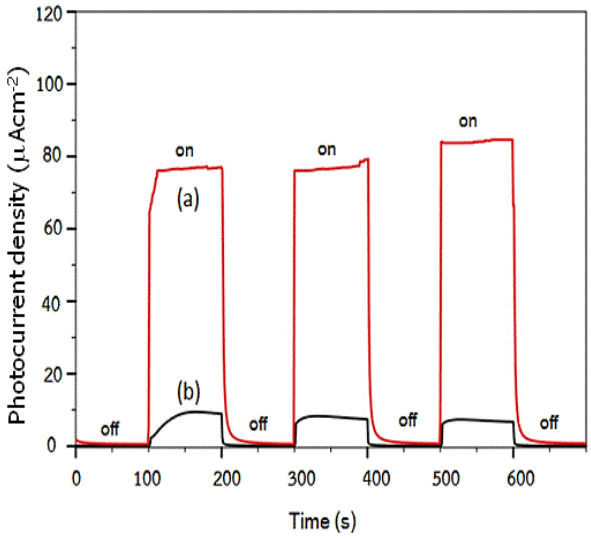

Figure 5 Photocurrent responses of (a) TNPs and (b) a CdS/TNPs photoanode under visible light irradiation in a 0.5M NaCl solution at 25°C. The illumination from a 11W compact florescence lamp (Sylvania, Daylight 865, $\lambda > 400$ nm) was interrupted every 100s.

TNPs and CdS/TNPs photoanodes recorded in 0.5 M NaCl. The current dropped to zero immediately when the light was cut off, and rose to the initial value again when the light was switched back on. This phenomenon indicates that the photoelectrochemical activity of the film electrode under irradiation resulted in the generation of a photocurrent. When a bare TNPs electrode is under light irradiation, the transient excitation current density reached ca. 9.47 μA cm^{-2} (Figure 5, curve a). While CdS/TNPs was used as the working electrode, the responsive photocurrent increased to ca. 83.8 μAcm^{-2} (Figure 5, curve b), which was approximately to 8.85 times higher than that of the bare TNPs electrode. This enhanced photocurrent response might have arisen from the doping of CdS into the TiO_2 nanoporous structure leading to faster charge transfer and more photogenerated charges that were effectively separated in the CdS/TNPs.

Figure 6a shows a schematic representation of the photocathodic protection method with the CdS/TNPs photoanode that generates electrons under visible light irradiation. This composite anode exhibits a transfer of photogenerated electrons from TiO_2 nanoporous particles to be stored by CdS nanocrystals. Then electrons are released slowly to the coupled 304SS, enhancing the photoelectric conversion efficiency. Therefore, the corrosion protection of metal can be achieved as long as a photo-effect is continued.

Figure 6b illustrates the mechanics of the improved charge separation of the CdS/TNPs photoanode under visible light irradiation. The electrons of both TiO_2 and CdS are photoexcited from the valence bands (VBs) to their corresponding conduction bands (CBs), leaving holes in the VBs. The excited electrons in the CB of CdS can be rapidly moved to the CB of TiO_2 which is situated below the CB of CdS. Finally, these electrons are transferred to 304SS. The result is that the photoelectrochemical performance of CdS/TNPs electrode induced by the low band gap energy excitation of electrons, separation of electron-hole pairs and the fast transport of mobile charges.

Figure 7a depicts a comparison of the open circuit potential OCP curve of 304SS coupled with the TNPs and CdS/TNPs electrodes under visible white light illumination and dark conditions. When illuminated by a UV light in the first period, it can be seen that the potential of both the 304SS coupled to TNPs and CdS/TNPs decreased quickly. This cathodic shift of the coupling potential resulted from the sudden creation of photoexcited electron-hole pairs and the transport of these electrons from the CdS/TNPs photoanodes onto the surface of the 304SS. Under the 1st illumination, the potential of the 304SS coupled to CdS/TNPs dropped immediately to a much more negative value (-471 mV versus SSE) than the initial dark potential of 304SS (-158 mV versus SSE). The more negative shift of the OCP curve implied that the photoanode exhibits more effective cathodic protection. Moreover, the potential of the 304SS coupled to CdS/TNPs was a more negative value than that of the 304SS coupled with TNPs under a dark condition. The light was turned off after 1 h of the 1st irradiation, the potential of the 304SS coupled with CdS/TNPs recovered only to a slightly less negative level than the noble value during 1 h under a dark condition. Then, the light was turned on and the electrode potential gradually shifted to the positive potential changed over 2 h of illumination. This negative electrode potential shift was still far below the E_{corr} of 304SS for the previous 4 h when the light was off, indicating the excess electrons stored in the CdS/TNPs structure were released and moved quickly to the 304SS. This implied that the catholic protection of 304SS can be maintained under dark conditions for quite a long time. In the case of a pure TNPs electrode, the photo-potential of 304SS coupled with TNPs changed immediately at each switching of illumination conditions due to fast recombination under visible-light illumination. The potential of 304SS coupled with TNPs shifted immediately to the negative value of -161 mV versus SSE, which was much less than that of 304SS coupled with CdS/TNPs. The photo-potential returned to greater positive values but was still below the dark potential of 304SS after the light was off. From these results, the CdS/TNPs film was superior to TNPs in effective cathodic protection for 304SS in a 0.5 M NaCl solution under illumination and dark conditions.

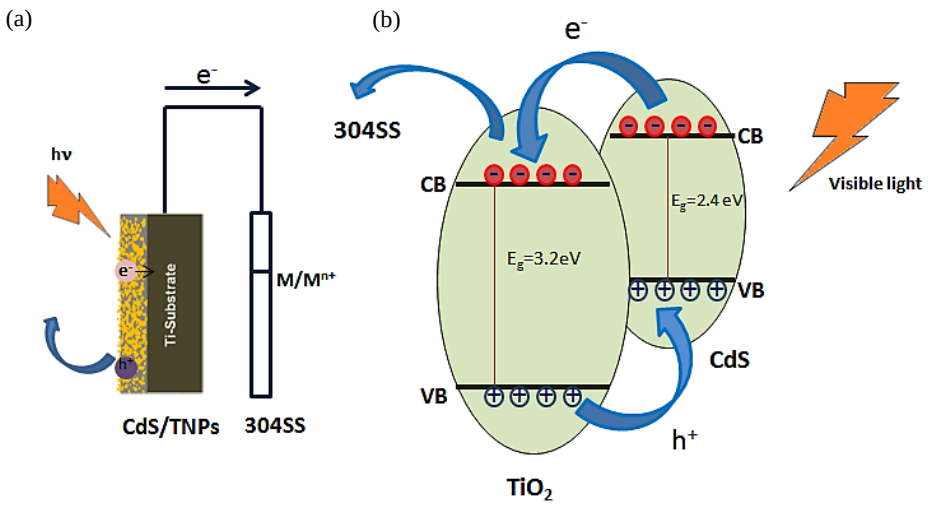

Figure 6 (a) Schematic representation of the photoelectrochemical metal anticorrosion system using a CdS/TNPs photoanode and (b) illustration of the energy band structure and electron-hole pair separation in the CdS/TNPs heterostructures.

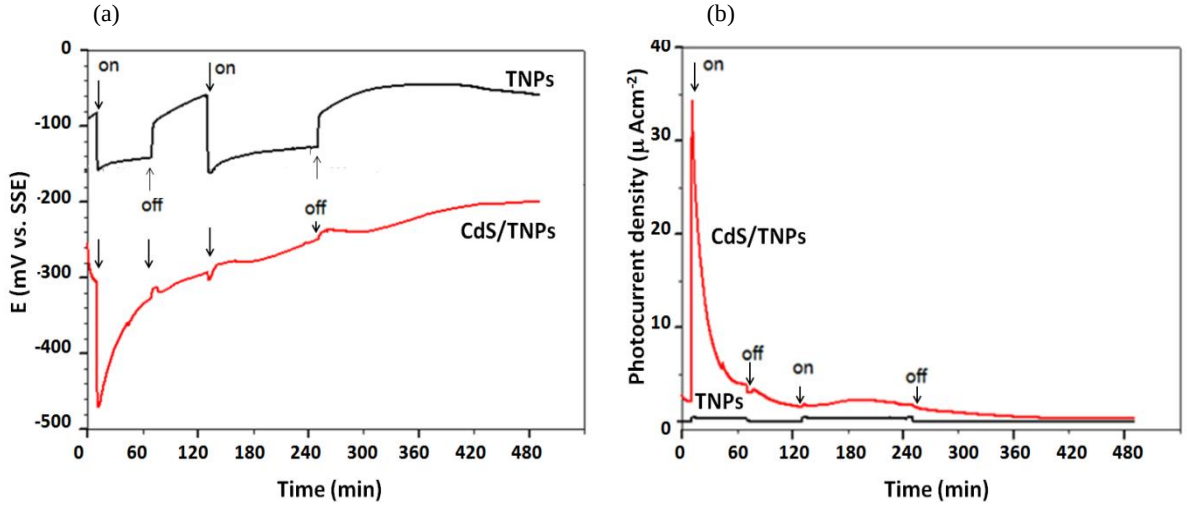

Figure 7 (a) The shift of the OCP, and (b) variations in currents with time under visible white light switched on and off for 304SS galvanic coupling with a TNPs or CdS/TNPs photoanode in a 0.5 M NaCl solution at 25°C.

Figure 7b shows the transient excitation current density comparison of 304SS coupling with TNPs or CdS/TNPs photoelectrodes under visible white light switched on and off. Starting under illumination, the photocurrent density reached maximum values of 4.3 and 34.3 μA cm^{-2} for the TNPs and CdS/TNPs samples, respectively. During the first hour-long illumination, the photocoupling current density of TNPs reached a relatively constant value, in contrast to that of CdS/TNPs sample, which sharply decreased. This phenomenon is caused by the equilibrium of competitive separation and recombination of photoexcited electron-hole pairs. Additionally, the photocoupling current density of CdS/TNPs fluctuated continuously during the remaining illumination/darkness cycles. A large number of mobile electrons were generated and transferred to the 304SS, maintaining cathodic protection. As seen in Figure 8, the surface morphologies of 304SS before and after being galvanic coupling with CdS/TNPs showed no corroded area on the metal surface in 0.5 M NaCl after visible white light was switched on for 8 h. This result shows that the 304SS was cathodically protected by CdS/TNPs coupling.

However, Figure 9 shows that the CdS film was destroyed and TiO_2 pores were corrupted after a galvanic coupling test in which there was penetration of chloride ions and an unstable CdS film. These defects were obvious when compared to the fresh CdS/TNPs (Figure 3b) that had a well arranged TiO_2 nanoporous film with some CdS nanocrystals dispersed inside the TiO_2 pores and smoothly covering the outside of the TNP film. In the case of 304SS coupled with TNPs, the photocurrent density dropped immediately after the light was turned off and reverted back to a less stable value due to the photoactive properties of titanium dioxide. The decrease of this current was caused by pitting and repassivation behavior and the 304SS was corroded even though it was coupled to the TNPs. It might be that the TNPs film was not dense enough to be used as a photoanode for metal protection in this study. That is why CdS decorated into the TNPs structure to decrease the energy band gap and increase the photogenerated electron-hole pairs. It is seen from Figure 7b that there is a small gap in the photocurrent density between CdS/TNPs and TNPs films for the last four hour-long dark condition.

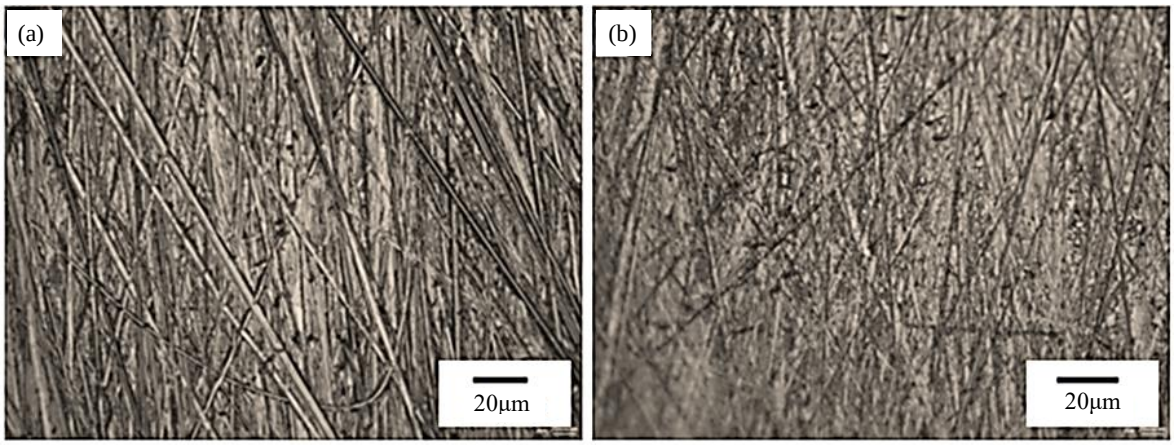

Figure 8 Top view FE-SEM image of 304SS (a) before and (b) 8 hr after, the photocatodic protection by CdS/TNPs

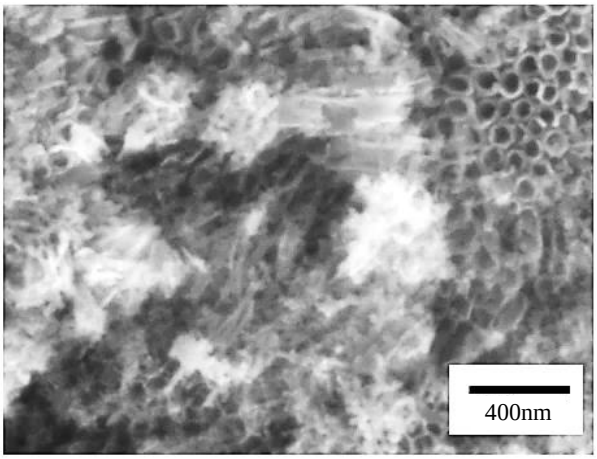

Figure 9 Top view FE-SEM image of the CdS/TNPs after 8 hr galvanic coupling to 304SS.

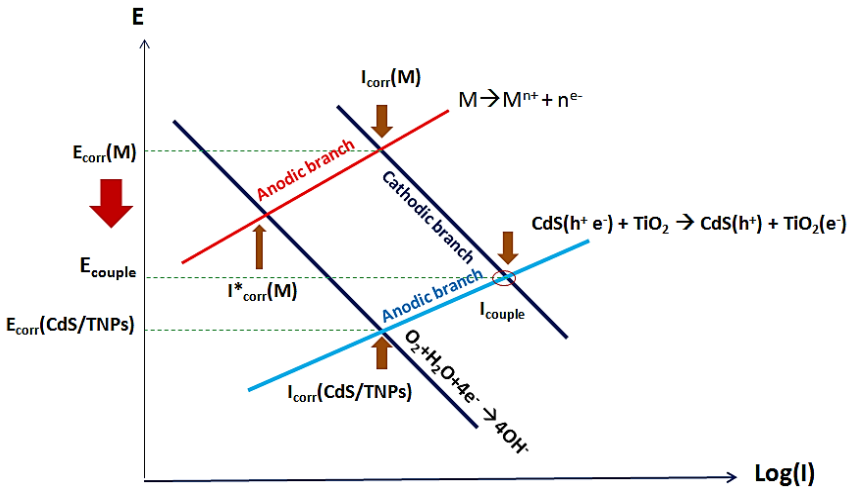

Figure 10 Evans diagrams explaining cathodic protection by galvanic coupling of metal (M) with a CdS/TNPs photoanode.

Electrochemical corrosion involves a reduction reaction of oxygen and/or water at a cathode, and an oxidation reaction or active dissolution at an anode. In this study, photocathodic protection is accomplished when the metal specimen becomes the cathode by galvanic coupling with the CdS/TNPs photoanode in a 0.5 M NaCl solution. From the galvanic polarization curves (Figure 10), the intersection of the reduction lines of oxygen and the oxidation line of metal or CdS/TNPs gives the corrosion potential of the metal (E_{corr} (M)) and that of CdS/TNPs (E_{corr} (CdS/TNPs)), respectively. Also the individual current density rates of the metal and CdS/TNPs are I_{corr} (M)) and I_{corr} (CdS/TNPs)), respectively. As a galvanic couple, these curves imply that the photogenerated electrons from a CdS/TNPs electrode flow to

the connected metal. Therefore, the potential is stabilized when total rate of oxidation equals the total rate of reduction. Figure 10 shows that the stabilized potential is lowered from E_{corr} (M) to E_{couple} and the coupling corrosion current density is depicted as I_{couple}. From this investigation, it could be summarized that the CdS/TNPs is much more negative than undecorated TNPs, which contributes to the existence of CdS in the TiO_2 nanoporous film due to the photogenerated electron-hole pairs. It is clear that when TiO_2 was doped with CdS, the polarization anodic current density was lower than that of TNPs and bare metal. This indicates that the corrosion rate of the 304SS was reduced when coupled with a CdS/TNPs electrode, resulting from the polarization of photogenerated electrons.

4. Conclusions

In this work, a CdS/TNPs film on a titanium substrate was prepared via a simple anodic oxidation method combined with a chemical bath deposition technique. CdS nanocrystals were distributed on the inside of nanopores and on the TiO_2 surface. Compared with the pure TNPs film, the photocurrent of the composite film was enhanced under visible light, indicating that CdS/TNPs was more efficient in developing photogenerated charge separation. Thus, the open circuit potentials of 304SS shifted to a negative value when coupled with a CdS/TNPs photoelectrode under an illuminated condition in a 0.5 M NaCl solution. Additionally, 304SS could still be protected for several hours even after illumination ceased. This indicates that the CdS-decorated TiO_2 nanoporous film has a potential application for cathodic protection of metals. Since the composite film was destroyed after polarization, further effort will be required to develop a stable and protective film.

5. Acknowledgements

We are grateful to the Faculty of Engineering, Khon Kaen University for the Master's degree student scholarship of Aleena Boonserm.

6. References

[1] Li H, Wang X, Liu Y, Hou B. Ag and SnO_2 co-sensitized TiO_2 photoanodes for protection of 304SS under visible light. Corrosion Sci. 2014;82:145-53.

[2] Pan C, Liu L, Li Y, Zhang B, Wang F. The electrochemical corrosion behavior of nanocrystalline 304 stainless steel prepared by magnetron sputtering. J Electrochem Soc. 2012;159(11):C453-60.

[3] Fu T, Zhou ZF, Zhou YM, Zhu XD, Zeng QF, Wang CP, et al. Mechanical properties of DLC coating sputter deposited on surface nanocrystallized 304 stainless steel. Surf Coating Tech. 2012;207:555-64.

[4] Li H, Bai X, Ling Y, Li J, Zhang D, Wang J. Fabrication of titania nanotubes as cathode protection for stainless steel. Electrochem Solid-State Lett. 2006;9(5):B28-31.

[5] Lei CX, Zhou H, Wang C, Feng ZD. Self-assembly of ordered mesoporous TiO_2 thin films as photoanodes for cathodic protection of stainless steel. Electrochim Acta. 2013;87:245-9.

[6] Li J, Lin CJ, Lin CG. A photoelectrochemical study of highly ordered TiO_2 nanotube arrays as the photoanodes for cathodic protection of 304 stainless steel. J Electrochem Soc. 2011;158(3):C55-62.

[7] Ali G, Chen C, Yoo SH, Kum JM, Cho SO. Fabrication of complete titania nanoporous structures via electrochemical anodization of Ti. Nanoscale Res Lett. 2011;6(1):1-10.

[8] Khomsab N. Effect of non-metal doping on the visible light photocatalytic activity of titanium dioxide. Ladkrabang engineering journal. 2013;30(2):19-24. [In Thai].

[9] Zhu YF, Xu L, Hu J, Zhang J, Du RG, Lin CJ. Fabrication of heterostructured $SrTiO_3/TiO_2$ nanotube array films and their use in photocathodic protection of stainless steel. Electrochim Acta. 2014;121:361-8.

[10] Park H, Bak A, Jeon TH, Kim S, Choi W. Photo-chargeable and dischargeable TiO_2 and WO_3 heterojunction electrodes. Appl Catal B Environ. 2012;115:74-80.

[11] Zhou MJ, Zeng ZO, Zhong L. Energy storage ability and anti-corrosion protection properties of TiO_2–SnO_2 system. Mater Corrosion. 2010;61(4):324-7.

[12] Zhang X, Tang Y, Li Y, Wang Y, Liu X, Liu C, et al. Reduced graphene oxide and PbS nanoparticles co-modified TiO_2 nanotube arrays as a recyclable and stable photocatalyst for efficient degradation of pentachlorophenol. Appl Catal Gen. 2013;457:78-84.

[13] Li J, Lin CJ, Li JT, Lin ZQ. A photoelectrochemical study of CdS modified TiO_2 nanotube arrays as photoanodes for cathodic protection of stainless steel. Thin Solid Films. 2011;519(16):5494-502.

[14] Jiang B, Yang X, Li X, Zhang D, Zhu J, Li G. Core-shell structure CdS/TiO_2 for enhanced visible-light-driven photocatalytic organic pollutants degradation. J Sol-Gel Sci Technol. 2013;66(3):504-11.

[15] Li W, Cui X, Wang P, Shao Y, Li D, Teng F. Enhanced photosensitized degradation of rhodamine B on CdS/TiO_2 nanocomposites under visible light irradiation. Mater Res Bull. 2013;48(9):3025-31.

[16] Li H, Wang X, Zhang L, Hou B. Preparation and photocathodic protection performance of CdSe/reduced graphene oxide/TiO_2 composite. Corrosion Sci. 2015;94:342-9.

[17] Wang Q, Yang X, Chi L, Cui M. Photoelectrochemical performance of CdTe sensitized TiO_2 nanotube array photoelectrodes. Electrochim Acta. 2013;91:330-6.

[18] Zhang J, Yang J, Liu M, Li G, Li W, Gao S, et al. Fabrication of CdTe quantum dots sensitized TiO_2 nanorod-array-film photoanodes via the route of electrochemical atomic layer deposition. J Electrochem Soc. 2014;161(1):D55-8.

[19] Lin ZQ, Lai YK, Hu RG, Li J, Du RG, Lin CJ. A highly efficient $ZnS/CdS/TiO_2$ photoelectrode for photogenerated cathodic protection of metals. Electrochim Acta. 2010;55(28):8717-23.

[20] Bessekhouad Y, Chaoui N, Trzpit M, Ghazzal N, Robert D, Weber JV. UV–vis versus visible degradation of Acid Orange II in a coupled CdS/TiO_2 semiconductors suspension. J Photochem Photobiol Chem. 2006;183(1):218-24.

[21] Peng T, Yang H, Dai K, Pu X, Hirao K. Fabrication and characterization of CdS nanotube arrays in porous anodic aluminum oxide templates. Chem Phys Lett. 2003;379(5):432-6.

[22] Wang C, Sun L, Yun H, Li J, Lai Y, Lin C. Sonoelectrochemical synthesis of highly photoelectrochemically active TiO_2 nanotubes by incorporating CdS nanoparticles. Nanotechnology. 2009;20(29):1-6.

[23] Zhang J, Du RG, Lin ZQ, Zhu YF, Guo Y, Qi HQ, et al. Highly efficient CdSe/CdS co-sensitized TiO_2 nanotube films for photocathodic protection of stainless steel. Electrochim Acta. 2012;83:59-64.
[24] Mallika T, Chaiyaput K. DSSCs fabrication using nano – structured titania as photoanode. Appl Mech Mater. 2015;781:184-8
[25] Mallika T, Chaiyaput K. Structural comparison of anodic nanoporous-titania fabricated from single-step and three-step of anodization using two paralleled-electrodes anodizing cell. KKU Eng J. 2015;43(1):13-20.

.